PROCEEDINGS A

royalsocietypublishing.org/journal/rspa

Research

Article submitted to journal

Subject Areas:
mechanobiology, soft tissues, applied mathematics

Keywords:
active remodeling, active stress, porous media, osmotic pressure, elasticity

Author for correspondence:
Insert corresponding author name
e-mail: davide.ambrosi@polito.it

Active over-relaxation and stress memory of living tissues after osmotic shock

P. Mascheroni[1], T. Boudou[1], G. Cappello[1], D. Ambrosi[2]

[1]Laboratoire Interdisciplinaire de Physique (LIPhy), Université Grenoble Alpes, CNRS, F-38000 Grenoble, France,[2] Dipartimento di Scienze Matematiche, Politecnico di Torino, Torino, Italy

Recent experiments show that a soft biological tissue generated by self–aggregation of different cell lines around two elastic pillars produces a traction that can be measured in terms of deflection of the beams themselves. When dextran is added to the fluid surrounding the tissue, an osmotic pressure applies on the sample which exhibits fast compression. On a longer timescale, about 30 minutes, the material elongates along the pillar inter-axis (the direction of active stress) up to a length that is even larger than the pre-shock one. We address an active mechanical explanation of such an unexpected behavior by investigating the peculiar poroelastic nature of the tissue material, made up of an active solid component that can remodel its dynamic activity on the basis of external loads.

1. Introduction

The idea of a mechanical cross-talk between cells and their environment dates back at least four centuries, with the preliminary intuitions of great scientists such as Galileo Galilei [1,2]. More recently, it has become clear that this state of dynamic reciprocity [3] plays a crucial role in several cellular phenomena, such as migration [4], differentiation [5] and progression in the cell cycle [6]. Moreover, alterations in the feedback loop between cells and their mechanical milieu have been shown to correlate with injuries and diseases [7]. Sometimes this cross-talk involves the tendency of cells to establish a target level of some mechanical quantity and keep it over time. This has been elucidated in tissue equivalents, i.e., in three-dimensional *in vitro* models of cells seeded in reconstituted fibrin or collagen matrices [8]. Such systems have clear advantages compared to *ex vivo* samples, in terms of reproducibility and ease of data acquisition. In the literature concerning these systems, the tendency of cells to seek a target state is generally known as 'tensional homeostasis' [2] and it has been shown to apply at different scales [9]. Over the years, the response of cells to changes in the environment that oppose maintenance of a target mechanical state has been a matter of vivid interrogation [10–14].

Recent experiments show that after a mechanical perturbation of a contractile soft tissue in homeostatic tensile state, the material returns in few minutes to a new equilibrium, intermediate between the original and the perturbed one [15]. In the same vein, the collective active tension produced by fibroblasts is reminiscent of the externally applied loads, depending on their application time [16]. On the other hand, osmotic pressure is a very effective tool to investigate the mechanobiology of biomaterials under compression, when a non trivial interplay between hydraulic and osmotic pressure occurs [17–20]. While there is a large literature devoted to investigate the mechanical behavior of living tissues under tensional external loads [2], the compressive case is much less understood. The reason of such a minor interest is probably not much in a minor physiological relevance, inasmuch an intrinsic technological difficulty that has been been recently addressed by the osmotic pressure [21].

In this work, we investigate theoretically at which extent a target state is modulated by changes in the mechanical environment of the cells populating tissue equivalents under compression. We show that the response of cells to a mechanical insult depends on active mechanisms that follow shortly from an early passive mechanical response. Using mathematical modeling, we propose a framework to account for such active mechanisms, disentangling the sequence of events that lead to the final state of the tissue.

2. The experiment

We specifically address the recent experiments by Giovanni Cappello et al. [22]. An uniaxially constrained tissue equivalent (microtissue, in the following) is seeded with NIH/3T3 cells between two pillars of known mechanical properties. A tracking algorithm records over time the evolution of the distance between pillars (L) and the tissue width (W), see Fig. 1. Knowing the pillar stiffness (k) and measuring their deflection it is possible to estimate the force exerted by the microtissue through the formula

$$F = -k(L - L_0), \tag{2.1}$$

L_0 being the distance between the unloaded pillars. After 24h from seeding, the microtissue is completely formed and bends the supporting pillars by exerting a force of a few μN. The value of this force is consistent across several tissues and slightly increases over time, as the cells compact more and more the intracellular collagen (see [22] for further details). It is possible to think of this force as the target, homeostatic mechanical state sought by the cells, which we will perturb in the following. Confocal images of the tissues reveal alignment of both collagen fibers and cell actin fibers in the direction along the pillars, showing the anisotropic organization within the cell aggregate (see Fig. 2a,b). At this time-point, an osmotic compression is applied to the

microtissue through the addition of dextran to the culture medium [18,19,21,23]. This results in a rapid compression (bump after the red arrow, Fig. 2c), followed by a later slower relaxation occurring over one hour. An elongation of the tissue eventually occurs along the longitudinal direction, as shown in Fig. 2d, with a compaction along the transverse direction. As a result, the tissue reaches a new (unexpected) target state in which the tension on the pillars is reduced compared to the state before the osmotic shock.

3. The mathematical model

To investigate the physics of the microtissue after addition of dextran, we formulate a mathematical model in which the aggregates are conceptualized as an active poroelastic material. The tissue is represented as a mixture of cells, extracellular matrix and interstitial fluid [19,24]. As the characteristic size of the cells and the extracellular matrix is much smaller than the macroscopic size of the sample, we model the aggregate as a porous material, constituted by a solid (cells and extracellular matrix) and (interstitial) fluid phases [25].

Before adding dextran to the culture medium, the external and internal fluid pressures are the same, and no fluid flow occurs through the pores of the solid phase. When dextran is added to the medium, it undergoes a fast diffusion in the surrounding fluid. Its molecular size prevents the diffusion of dextran into the interstitial space [18]. The small pores at the tissue boundary act therefore as a semipermeable membrane, and the osmotic pressure difference generates a fluid outflow towards a new thermodynamical equilibrium. The dynamics leading to pressure equilibrium follow a diffusion process characterized by the hydraulic diffusion coefficient

$$D_h \sim \tilde{k}(2\mu + \gamma)/\tilde{\mu}, \tag{3.1}$$

where $\tilde{k}$ is the tissue permeability, μ and γ are the shear modulus and Lamé constant of the aggregate, and $\tilde{\mu}$ is the extra-cellular fluid viscosity [19,26]. Considering a permeability $\tilde{k} \sim 10^{-18}\,\mathrm{m}^2$ [19], a shear and Lamé moduli of $10\,\mathrm{kPa}$, and a viscosity $\tilde{\mu} \sim 10^{-3}\mathrm{Pa}\cdot\mathrm{s}$, the diffusion scaling $t^* \sim L^2/D_h$ suggests a timescale t^* for water percolation of the order of a few minutes for aggregates of a few hundreds of microns in size. This is consistent with the compression bump seen in Fig. 2 and with the observations for single cells reported in Ref. [27].

If the dextran macromolecules are big enough [22], they do not enter the interstitial space of the porous medium and, at steady state, the Kedem-Katchalski condition [28] (the continuity of chemical potential) applies across the boundary of the tissue, i.e.,

$$p = -\pi, \tag{3.2}$$

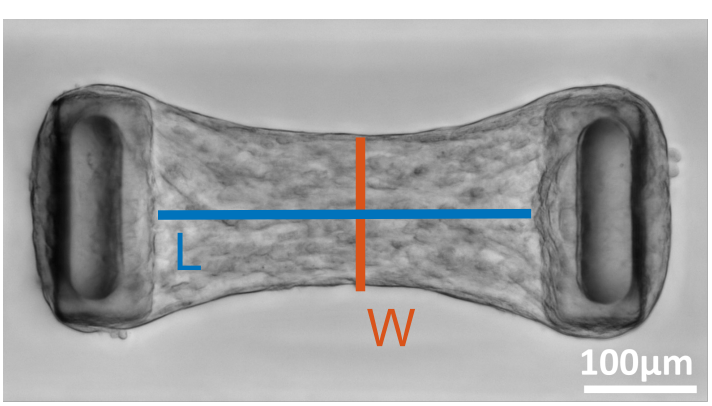

Figure 1. Image of a reference 3T3 microtissue before osmotic compression. The length between the pillars (L) and the tissue width (W) are used to characterize the morphological modifications of the microtissues during the experiments.

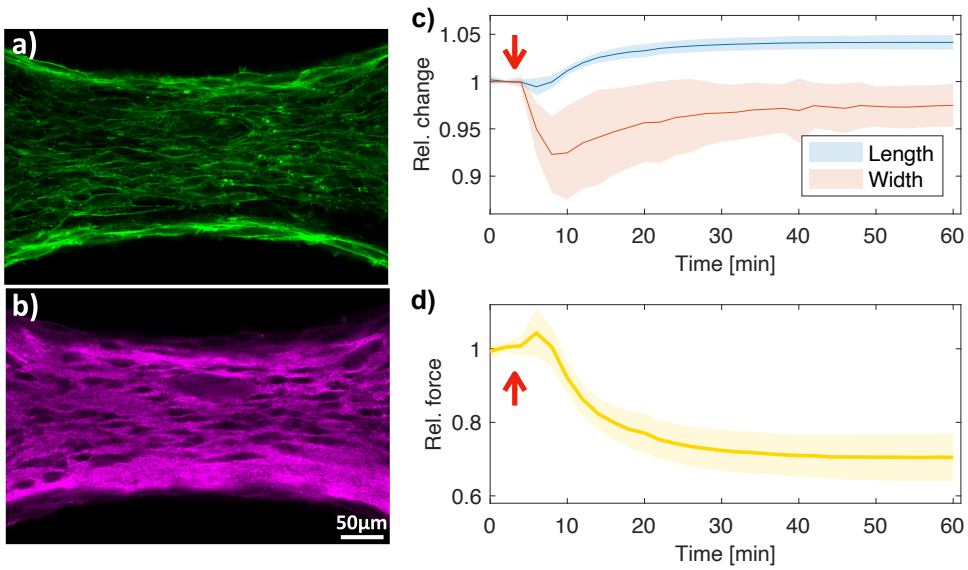

Figure 2. Confocal images of a representative 3T3 microtissue, stained for actin (a) and collagen (b). The images highlight the anisotropic orientation of fibers along the longitudinal pillar-to-pillar axis

. After an osmotic compression of 5kPa (red arrow), the tissue relaxes the tension exerted on the pillars (c). This corresponds to an elongation along the direction of the pillars and a small reduction of the width along the transverse direction (d). The reference quantities used to calculate the relative changes are the defined at the beginning of the experiment, before applying the osmotic compression. The lines in (c,d) are the mean of individual experiments, shaded areas represent the standard deviation. The results are the mean $\pm$ Standard Deviation of n > 50 microtissues from N = 3 experiments.

where p is the interstitial fluid pressure, $\pi > 0$ is the osmotic pressure generated by the dextran molecules [19], the surrounding fluid pressure being taken equal to zero.
The total stress [26] in the poroelastic medium is given by the sum of the solid stress T and fluid pressure: as the tissue is mechanically unloaded at the boundary, it holds

$$\mathsf{T} - p\mathsf{I} = 0, \tag{3.3}$$

and the stress in the solid phase at the boundary reads

$$\mathsf{T} = p\mathsf{I} = -\pi\mathsf{I}, \tag{3.4}$$

and the osmotic pressures loads the solid component of the mixture only.
The constitutive law for the solid stress is formulated in terms of the active strain theory [29,30]. We start by prescribing the following strain energy density for the material

$$W(\mathsf{F}_e) = \frac{\mu}{2}\left(\mathsf{F}_e : \mathsf{F}_e - 2\log J_e - 3\right) + \frac{\gamma}{2}(J_e - 1)^2 + \frac{\alpha}{4}\left(\mathsf{F}_e\mathbf{n}\cdot\mathsf{F}_e\mathbf{n} - 1\right)^2, \tag{3.5}$$

where $J_e = \det(\mathsf{F}_e)$ and F_e represent the elastic part of the total deformation. According to the multiplicative decomposition [31]

$$\mathsf{F}_e = \mathsf{F}\mathsf{G}^{-1}. \tag{3.6}$$

where $\mathsf{F} = \frac{\partial \mathbf{x}(\mathbf{X},t)}{\partial \mathbf{X}}$ and the motion function $\mathbf{x}(\mathbf{X},t)$ provides the position at time t of the material point that was in $\mathbf{X}$ at time $t = 0$. The tensor G accounts for the active cell contraction in the microtissue [30]: the ability of the tissue to re-establish tensional homeostasis after a mechanical

insult [2], possibly towards a target modulated by a previous perturbation [29]. For $\mathsf{G}=\mathsf{I}$ (no activity), one recovers in Eq. (3.5) a standard compressible hyperelastic material of Neo-Hookean type [32]: the strain energy is the sum of a classical quadratic term, a logarithmic barrier that inhibits access to the region $\det \mathsf{F} \leq 0$, a quadratic penalization in volumetric variation and an anisotropic contribution that accounts for alignment of the fibers. In the limit of infinitesimal strains, μ and γ are the shear modulus and Lamé parameter, respectively. For soft living matter, typically $\mu,\ \gamma \sim 1-30\,\mathrm{kPa}$ [33]. The value for γ takes into account the presence of pores in the solid phase (i.e., it is a *drained* modulus [26]), leading to moderate values of compressibility. Then, the unit vector $\mathbf{n}$ is aligned with the axis of the pillars, whereas α is an anisotropic shear modulus accounting for the collagen fibers. Typically, $\alpha > \mu$.
From the strain energy (3.5) we can derive the Cauchy stress

$$\mathsf{T} = J_e^{-1}\frac{dW}{d\mathsf{F}_e}\mathsf{F}_e^{\mathsf{T}}, \tag{3.7}$$

which, according to Eq. (3.6), reads

$$\begin{aligned}\mathsf{T} = \quad & \frac{\mu J_g}{J}\left(\mathsf{F}\mathsf{G}^{-1}\mathsf{G}^{-\mathsf{T}}\mathsf{F}^{\mathsf{T}}-\mathsf{I}\right)+\gamma\left(\frac{J}{J_g}-1\right)\mathsf{I}+\\ & \frac{\alpha J_g}{J}\left(\mathsf{F}\mathsf{G}^{-1}\mathbf{n}\cdot\mathsf{F}\mathsf{G}^{-1}\mathbf{n}-1\right)\mathsf{F}\mathsf{G}^{-1}\mathbf{n}\otimes\mathsf{F}\mathsf{G}^{-1}\mathbf{n}.\end{aligned} \tag{3.8}$$

The symmetry of the problem suggests to look for a homogeneous deformation solution of the type

$$\mathsf{F}=\mathrm{diag}\{\lambda_1,\lambda_2,\lambda_2\}, \qquad \mathsf{G}=\mathrm{diag}\{a,b,b\}, \tag{3.9}$$

in which λ_1 and λ_2 are the relative change in length and width of the microtissue, whereas a and b represent the longitudinal and transverse components of active remodeling, respectively. The force balance equations in spatial coordinates read

$$T_{11} = -\pi - \kappa(\lambda_1 - 1), \tag{3.10a}$$

$$T_{22} = -\pi, \tag{3.10b}$$

where $\mathbf{n}=(1,0,0)^T$. Here, κ is the rescaled stiffness of the pillars; independent experiments measure a rigidity $K=0.5\,\mathrm{Nm}^{-1}$, see Eq. (2.1). We can derive $\kappa = KL_0/A_0$, where A_0 is the area of the tissue section. For these tissues, we estimate $\kappa \sim 5\,\mathrm{kPa}$. By using the ansatz in (3.9), the algebraic system of equations to solve reads

$$\mu\frac{ab^2}{\lambda_1\lambda_2^2}\left(\frac{\lambda_1^2}{a^2}-1\right)+\gamma\left(\frac{\lambda_1\lambda_2^2}{ab^2}-1\right)+\alpha\frac{ab^2}{\lambda_1\lambda_2^2}\left(\frac{\lambda_1^2}{a^2}-1\right)\frac{\lambda_1^2}{a^2} = -\pi-\kappa(\lambda_1-1), \tag{3.11a}$$

$$\mu\frac{ab^2}{\lambda_1\lambda_2^2}\left(\frac{\lambda_2^2}{b^2}-1\right)+\gamma\left(\frac{\lambda_1\lambda_2^2}{ab^2}-1\right) = -\pi. \tag{3.11b}$$

As a final step, we need to specify governing equations for the active components a and b. We take inspiration from the literature for active remodeling in finite deformations [34], and formulate an evolution law that depends on some measure $\mathcal{F}(\mathsf{T})$ of the tensional state in the microtissue and its history. Regarding the temporal dynamics, the experimental curves in Figs. 2c,d reveal that, after the osmotic shock, the tissue relaxes in a timescale of 20-30 minutes up to strains that are different from the pre-shock ones; notably the final longitudinal strain is even larger than the pre-shock one. This time scale is in agreement with the active reorganization time-scale of single cells [27,35] and with the relaxation time of tissue equivalents subject to stress relaxation experiments [14]. The existence of a relaxation time yields a memory effect, which can be introduced in the equations in a way similar to what is known for viscoelastic materials [36,37]. Classical theory suggests an

evolution equation of the type

$$\frac{d\mathsf{G}}{dt} = -\frac{1}{t_r}\left(\mathsf{G} - (\mathsf{I} + \mathsf{A}\mathcal{F}(\mathsf{T}))\right) \tag{3.12}$$

with the memory functional

$$\mathcal{F}(\mathsf{T}) = \int_0^t \frac{d}{dt'}\left(\mathsf{T}(t') \cdot \mathsf{I}\right) e^{-(t-t')/t_m}\, dt', \tag{3.13}$$

where the temporal derivative of the trace of the Cauchy stress in the solid phase is modulated by an exponential kernel with a characteristic time t_m, I is the identity tensor and A is a constant symmetric positive definite tensor. Since dextran compresses the tissue on a timescale much shorter than the development of active effects (as per Eq. (3.1)), we approximate the derivative of the stress with a Kronecker delta centered at the time of the osmotic shock t_s, i.e.,

$$\frac{d\left(\mathsf{T}(t) \cdot \mathsf{I}\right)}{dt} \sim -\pi\delta(t - t_s). \tag{3.14}$$

The approximation in Eq. (3.14) leads to

$$\mathcal{F}(\mathsf{T}) \sim -\pi e^{-(t-t_s)/t_m}. \tag{3.15}$$

Assuming that the characteristic time t_m is much longer than the duration of the experiment (i.e., $t_m \gg t - t_s$), the system of equations (3.12) eventually rewrites

$$\frac{da}{dt} = -\frac{1}{t_r}\left[a - \left(1 + \beta\frac{\pi}{\alpha}\right)\right], \tag{3.16a}$$

$$\frac{db}{dt} = -\frac{1}{t_r}\left[b - \left(1 + r\frac{\pi}{\alpha}\right)\right], \tag{3.16b}$$

where t_r is a common relaxation time, set to 10 min, in agreement with the experiments in Ref. [14,35] and $\mathsf{A} = \mathrm{diag}(\beta/\alpha, r/\alpha, r/\alpha)$, thus reflecting the anisotropy of the material. The nondimensional constant r modulates the transverse versus longitudinal remodelling. The rationale behind equations (3.16) is that the well known ability of living tissues to actively organize an homeostatic stress state [30] may depend on the recent tensional history of the sample; we assume that the new homeostatic stress depends on the peak stress experienced by the tissue along a past time interval (namely π in the present framework). The factor β accounts for the modulation of active tension possibly produced by blebbistatin: $\beta = 1$ is the control, $\beta = 0.4$ when blebbistatin is added. Blebbistatin is an inhibitor of the actomyosin contractility in cells; however it does only partially switches off the mechanical activity. The non null value of β that we adopt is proportional to the residual active tension after delivery of the inhibitor.

Remark A key unconventional aspect of the experiments we address is that the living material, the multicellular sample, does not exist in a former relaxed state: aggregation and activity develop simultaneously. The cells plugged in the culture medium aggregate, they attach to the cantilevers, they form a multicellular porous material and, at the same time, they generate tension. This is not usual even in classical biomechanics: when a muscle is electrically stimulated, active tension is produced, it can be electrically controlled and the strain of the muscle can be compared with the original (relaxed) one.

What we know in our setup, under assumption of homogeneous deformation, are the longitudinal and transverse stress, because we know that the sample is transversely unloaded and we know the deflection of the cantilevers. We measure a force on the nanopillars of about 11 μN (CTRL) and 5 μN (with blebbistatin). If we had some information on the strain of the material before the osmotic shock, we could place ourselves in the correct point of the stress-strain curve, but unfortunately we do not. In other words, we do not know F_e and G at time $t = 0$, before the osmotic shock, but we assume that initially $\mathsf{F} = \mathsf{F}_e\mathsf{G} = \mathsf{I}$: we do not know in which position of the stress-strain curve we are at time $t = 0$ and we place ourselves in the origin.

Table 1. Values of the parameters used for the simulations.

Parameter	Value	Unit	Description
κ	5	kPa	Stiffness of elastic pillars
π	5	kPa	Osmotic shock
μ	10	kPa	Bulk shear modulus
γ	10	kPa	Bulk Lamé constant
α	100	kPa	Anisotropic shear modulus
t_r	10	min	Relaxation time
β	1-0.4	-	Blebbistatin modulation of activity
r	2	-	longitudinal vs transverse remodeling

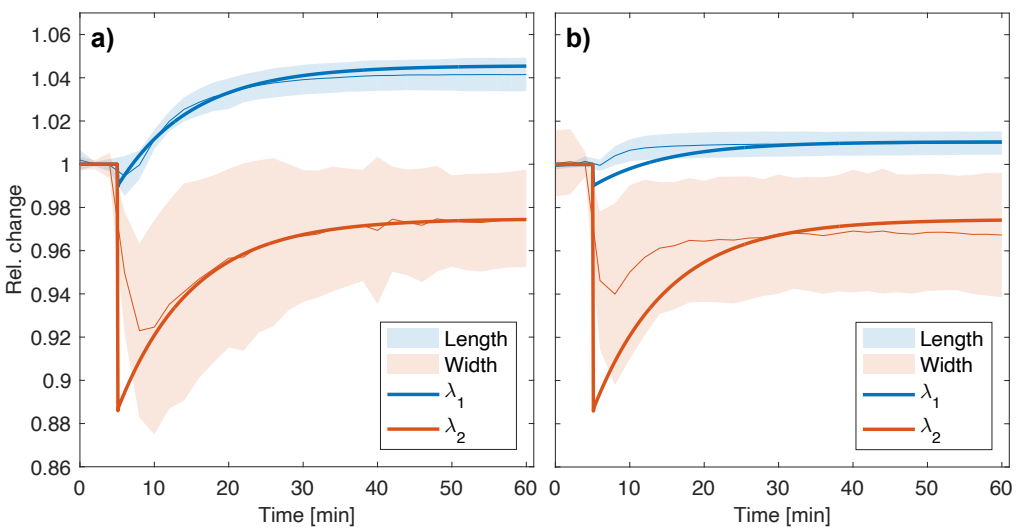

Figure 3. Comparison between experimental curves and model predictions, for tissues grown in standard conditions (a) and in the presence of blebbistatin (b). The osmotic shock takes place after 5 min (red arrow) from the beginning of the experiment. Thin lines represent the mean of the experiments, shaded areas the standard deviation. Thick lines show model predictions.

4. Results

We solve the system in Eqs. (3.11),(3.16) using the parameters in Table 1. Fig. 3 shows a comparison between experiments and theoretical predictions. We take the reference configuration $\mathsf{F} = \mathsf{I}$ in the material at time $t = 0$. Such a configuration is not stress-free and, as a matter of fact, the zero stress configuration is unknown in our device because the tissue arises in a tensional state from the very beginning: cell aggregation and generation of active tension occur simultaneously. In principle the relaxed state could be devised detaching the cells from the pillars and inhibiting the cell activity, but this is immaterial for our purposes. Both the fast compression, immediately after the osmotic shock (red arrow in Fig. 3a), and the slow relaxation are well captured.

The material is longitudinally stiffer and its strain competes energetically with the work of active and elastic external forces (the pillars). We remark that a simpler recovery law along one direction only could not reproduce the longitudinal over-relaxation reported in the experimental data, not even for auxetic materials, in which axial elongation causes transversal elongation [38]. No purely passive viscoelastic lumped-parameters models (e.g., [13]) can reproduce the curve for λ_1 in

Fig. 3a: relaxation possibly takes back to a tensional state equal to the initial one, the observed over-relaxation is of active nature. In the same vein, no nonlinear elastic material can account for the observed elongation under load: even for a non-convex strain energy, the monotonicity of the strain-stress relation abides under load, possible hysteresis shows up in the unloading phase only (see also the discussion in Appendix).

The experimental evidence that the response to the osmotic shock is due to active effects, is provided by exposition of the microtissues to blebbistatin, a myosin-II inhibitor, for 1 h before performing the osmotic shock. Fig. 3b shows that, by inhibiting active responses, the tissues are not able to over-relax their lengths, nor to recover the transverse compaction.

Most of the data that we have that we have from experiments are phenomenological in the sense that they provide information at a tissue, macroscopic level. Partial knowledge at a molecular level can be be inferred from the longitudinal orientation of actin, reported in Figure 2: cells elongated longitudinally exert stress in the direction of actin alignment. While we have not experimentally devised the pattern of myosin activity (the molecular motors that generate active tension), we know that they glide along actin fibres, so that the orientation of the latter determines the (main) orientation of the the active stress. In the same vein, we know that after inhibition of myosin the observed super-relaxation vanishes, and this is the signature of an active behavior. We might also argue about a possible role for the orientation of actin fibers dictated by osmotic compression: compression might induce a less aligned configuration of fibres, thus making the force generated by the myosin molecules less effective. It is consensually accepted that cells contract more on stiff substrates than on soft ones, and they change shape accordingly [39]. In addition, we have seen similar results when we compressed the ECM around the cells [18]. However, at this stage of experimental evidence, these are only speculations about the cell-level origin of the observed behavior and we keep the modeling at a macroscopic level.

In conclusion, we have discussed the mechanism such that a microtissue sample attached to flexible pillars reacts to an osmotic shock by an active (long time) relaxation after the initial (short time) passive compression. The osmotic pressure applies in a range (around 5 KPa) that does not significantly affect the volume and morphology of single cells, thus supporting the importance to model the system as a mixture of cells and extracellular matrix [18]. Such active behavior drives the tissue to a new tensional equilibrium over-relaxing the initial length and such that the initial width is only partially recovered. Using mathematical modeling, we account for both these anisotropic mechanisms. First, cells align their cytoskeleton along the direction of the pillars in a way that accommodates the external pressure, as previously seen for example in [21,22]. Second, cells counterbalance the osmotic pressure partially recovering the deformation in the transverse direction (i.e., orthogonal to the line joining the pillars). A similar behavior is shown in microtissues that, after displacement from their homeostatic mechanical state, generate an active response that opposes the external loading [13,14]. Our results support the idea that the target, homeostatic, tensional state actively sought by cells can be altered by external perturbations: the target stress is influenced by its tensional history. This raises questions about the encoding of such target state in 'cell memory' [40] and about the biological mechanisms that lead to its modulation via the cross-talk with the mechanical environment.

Acknowledgements. DA acknowledges the support of the *Gruppo Nazionale di Fisica Matematica* of the INDAM. PM acknowledges financial support from the Marie Sklodowska-Curie Individual Fellowship for the Project CHECKMATE (Grant Nr. 893981). TB acknowledges funding from the ANR CONTRACTILE project, grant ANR-23-CE13-0037 of the French ANR.

Appendix

Consider a continuum body subject to a constant pressure p at its boundary; then in any point of the boundary $\mathsf{T}\mathbf{n} = -p\mathbf{n}$, where T denotes the Cauchy stress tensor and $\mathbf{n}$ is the normal outgoing unit vector. A possible characterization of an admissible strain energy $W(\mathsf{F})$ is to require that it

satisfies the rank-one convexity condition [41]:

$$\left(\frac{\partial W}{\partial \mathsf{F}}(\bar{\mathsf{F}}+\delta\mathsf{F})-\frac{\partial W}{\partial \mathsf{F}}(\bar{\mathsf{F}})\right):\delta\mathsf{F}>0 \tag{4.1}$$

for every dyadic tensor $\delta\mathsf{F}$. In particular, for an homogeneous diagonal deformation, the monotonicity condition (4.1) yields that the sign of stress and strain increment must be the same, so that under compression the lengths shorten.

The possible introduction of viscoelasticity [42] does not modify the argument above, neither in the transient nor at equilibrium. For example, in a Kelvin-Voigt solid the equilibrium state, according to the force balance under applied load, is reached in a relaxation time dictated by the viscous damping: however the inequality above is not violated neither in the transient nor at equilibrium. More sophisticated viscoelastic models like standard solid behave in the same qualitative way, according to more than one relaxation time. Fluid-like models (like the Maxwell fluid) predict an unbounded relaxation flow that is not in agreement with observations.

We eventually mention that we have also worked out an example of elastic but not hyperelastic material, such that the Cauchy stress is directly provided as a function of the strain and cannot descend from variation of a strain energy. This model is able to account for the observed elongation under compression. However, an elastic stress tensor that does not follow from variation of a strain energy typically exhibits hysteresis, an anelastic behavior that, in our opinion, is better captured by the active strain approach that we follow here.

Supplementary Material

The data that support the findings of this article are openly available in
Mascheroni P, Boudou T, Cappello G, and Ambrosi D.(2025). Supplementary materials for the article "Active over-relaxation and stress memory of living tissues after osmotic shock" (1.0) [Data set]. Zenodo. https://doi.org/10.5281/zenodo.17459443

References

1. Cyron C, Humphrey J. 2017 Growth and remodeling of load-bearing biological soft tissues. *Meccanica* **52**, 645–664.
2. Eichinger JF, Haeusel LJ, Paukner D, Aydin RC, Humphrey JD, Cyron CJ. 2021 Mechanical homeostasis in tissue equivalents: a review. *Biomechanics and modeling in mechanobiology* **20**, 833–850.
3. Bissell M, Aggeler J. 1987 Dynamic reciprocity: how do extracellular matrix and hormones direct gene expression?. *Progress in clinical and biological research* **249**, 251–262.
4. Gupton SL, Waterman-Storer CM. 2006 Spatiotemporal feedback between actomyosin and focal-adhesion systems optimizes rapid cell migration. *Cell* **125**, 1361–1374.
5. Maître JL, Turlier H, Illukkumbura R, Eismann B, Niwayama R, Nédélec F, Hiiragi T. 2016 Asymmetric division of contractile domains couples cell positioning and fate specification. *Nature* **536**, 344–348.
6. Delarue M, Montel F, Vignjevic D, Prost J, Joanny JF, Cappello G. 2014 Compressive stress inhibits proliferation in tumor spheroids through a volume limitation. *Biophysical journal* **107**, 1821–1828.
7. Huang S, Ingber DE. 2005 Cell tension, matrix mechanics, and cancer development. *Cancer cell* **8**, 175–176.
8. Polacheck WJ, Chen CS. 2016 Measuring cell-generated forces: a guide to the available tools. *Nature methods* **13**, 415–423.
9. Stamenović D, Smith ML. 2020 Tensional homeostasis at different length scales. *Soft Matter* **16**, 6946–6963.
10. Brown R, Prajapati R, McGrouther D, Yannas I, Eastwood M. 1998 Tensional homeostasis in dermal fibroblasts: mechanical responses to mechanical loading in three-dimensional substrates. *Journal of cellular physiology* **175**, 323–332.

11. Ezra DG, Ellis JS, Beaconsfield M, Collin R, Bailly M. 2010 Changes in fibroblast mechanostat set point and mechanosensitivity: an adaptive response to mechanical stress in floppy eyelid syndrome. *Investigative ophthalmology & visual science* **51**, 3853–3863.
12. Walker M, Rizzuto P, Godin M, Pelling AE. 2020a Structural and mechanical remodeling of the cytoskeleton maintains tensional homeostasis in 3D microtissues under acute dynamic stretch. *Scientific reports* **10**, 1–16.
13. Walker M, Godin M, Harden JL, Pelling AE. 2020b Time dependent stress relaxation and recovery in mechanically strained 3D microtissues. *APL bioengineering* **4**, 036107.
14. Eichinger JF, Paukner D, Szafron JM, Aydin RC, Humphrey JD, Cyron CJ. 2020 Computer-controlled biaxial bioreactor for investigating cell-mediated homeostasis in tissue equivalents. *Journal of biomechanical engineering* **142**, 071011.
15. Eichinger JF, Paukner D, Aydin RC, Wall WA, Humphrey JD, Cyron CJ. 2021 What do cells regulate in soft tissues on short time scales?. *Acta biomaterialia* **134**, 348–356.
16. Hong Y, Peng X, Yu H, Jafari M, Shakiba D, Huang Y, Qu C, Melika EE, Tawadros AK, Mujahid A, Sandler J, Pryse KM, Sacks JM, Elson EL, Genin GM, Alisafaei F. 2023 Matrix Softening Controls Stretch-Induced Cellular Memory and Fibroblast Activation. *bioRxiv*. (10.1101/2022.10.12.511903)
17. Ambrosi D, Pezzuto S, Riccobelli D, Stylianopoulos T, Ciarletta P. 2017 Solid tumors are poroelastic solids with a chemo-mechanical feedback on growth. *Journal of Elasticity* **129**, 107–124.
18. Dolega ME, Monnier S, Brunel B, Joanny JF, Recho P, Cappello G. 2021a Extracellular matrix in multicellular aggregates acts as a pressure sensor controlling cell proliferation and motility. *Elife* **10**, e63258.
19. Dolega M, Zurlo G, Le Goff M, Greda M, Verdier C, Joanny JF, Cappello G, Recho P. 2021b Mechanical behavior of multi-cellular spheroids under osmotic compression. *Journal of the Mechanics and Physics of Solids* **147**, 104205.
20. Kourouklis AP, Wahlsten A, Stracuzzi A, Martyts A, Paganella LG, Labouesse C, Al-Nuaimi D, Giampietro C, Ehret AE, Tibbitt MW et al.. 2023 Control of hydrostatic pressure and osmotic stress in 3D cell culture for mechanobiological studies. *Biomaterials Advances* **145**, 213241.
21. Dolega M, Delarue M, Ingremeau F, Prost J, Delon A, Cappello G. 2017 Cell-like pressure sensors reveal increase of mechanical stress towards the core of multicellular spheroids under compression. *Nature communications* **8**, 1–9.
22. Cappello G, Wodrascka F, Marquez-Vivas G, Radwan AE, Anoop P, Mascheroni P, Fouchard J, Fabry B, Ambrosi D, Recho P et al.. 2025 Osmotic pressure induces unexpected relaxation of contractile 3D microtissue. *The European Physical Journal E* **48**, 34.
23. Montel F, Delarue M, Elgeti J, Malaquin L, Basan M, Risler T, Cabane B, Vignjevic D, Prost J, Cappello G et al.. 2011 Stress clamp experiments on multicellular tumor spheroids. *Physical review letters* **107**, 188102.
24. Preziosi L. 2003 *Cancer modelling and simulation*. CRC Press.
25. Bell S, Ackermann J, Maitra A, Voituriez R. 2025 Ordering spontaneous flows and aging in active fluids depositing tracks. *Phys. Rev. E* **111**, L023405. (10.1103/PhysRevE.111.L023405)
26. Cheng AHD. 2016 *Poroelasticity* vol. 27. Springer.
27. Cadart C, Venkova L, Recho P, Lagomarsino MC, Piel M. 2019 The physics of cell-size regulation across timescales. *Nature Physics* **15**, 993–1004.
28. Kedem O, Katchalsky A. 1958 Thermodynamic analysis of the permeability of biological membranes to non-electrolytes. *Biochimica et biophysica Acta* **27**, 229–246.
29. Ambrosi D, Pezzuto S. 2012 Active stress vs. active strain in mechanobiology: constitutive issues. *Journal of Elasticity* **107**, 199–212.
30. Taber LA. 2009 Towards a unified theory for morphomechanics. *Philosophical Transactions of the Royal Society A: Mathematical, Physical and Engineering Sciences* **367**, 3555–3583.
31. Gurtin ME. 1982 *An introduction to continuum mechanics*. Academic press.
32. Ogden RW. 1997 *Non-linear elastic deformations*. Courier Corporation.
33. Zhao R, Boudou T, Wang WG, Chen CS, Reich DH. 2013 Decoupling cell and matrix mechanics in engineered microtissues using magnetically actuated microcantilevers. *Advanced materials* **25**, 1699–1705.
34. Ambrosi D, Guana F. 2007 Stress-modulated growth. *Mathematics and mechanics of solids* **12**, 319–342.
35. Jiang H, Sun SX. 2013 Cellular pressure and volume regulation and implications for cell mechanics. *Biophysical journal* **105**, 609–619.

36. Boltzmann L. 1878 Zur theorie der elastischen nachwirkung. *Annalen der Physik* **241**, 430–432.
37. Dautray R, Lions JL. 2012 *Mathematical analysis and numerical methods for science and technology: volume 1 physical origins and classical methods*. Springer Science & Business Media.
38. Papadopoulou A, Laucks J, Tibbits S. 2017 Auxetic materials in design and architecture. *Nature Reviews Materials* **2**, 1–3.
39. Yeung T, Georges PC, Flanagan LA, Marg B, Ortiz M, Funaki M, Zahir N, Ming W, Weaver V, Janmey PA. 2005 Effects of substrate stiffness on cell morphology, cytoskeletal structure, and adhesion. *Cell Motility* **60**, 24–34. (https://doi.org/10.1002/cm.20041)
40. Nasrollahi S, Walter C, Loza AJ, Schimizzi GV, Longmore GD, Pathak A. 2017 Past matrix stiffness primes epithelial cells and regulates their future collective migration through a mechanical memory. *Biomaterials* **146**, 146–155.
41. Antman S. 2005 *Nonlinear Problems of Elasticity*. Springer.
42. Flügge W. 1975 *Viscoelasticity*. Raymond F. Boyer Library Collection. Springer-Verlag.